Research Article

Journal of Environmental Nanotechnology

# Investigation of Metakaolin Utilization as a Supplement to Cement in Sustainable High-performance Concrete Production

S. Jagan*, N. Kiruthiga, R. Ramya, S. N. Shri Hariharan and S. Jagadeesh
Department of Civil Engineering, Sona College of Technology, Salem, TN, India
Received: 30.12.2024 Accepted: 18.02.2025 Published: 30.03.2025
*kecjagan@gmail.com

## ABSTRACT

The research on the use of supplementary cementitious materials in enhancing the behavior of high-performance concrete (HPC) has increased. This paper investigates the influence of metakaolin (MK) on the properties of the HPC; cement was substituted with 5, 10, 15, 20, 25, and 30% of MK by weight to manufacture HPC at lower and higher w/b ratios. The concrete mixtures were evaluated for their fresh properties through compaction factor test and mechanical properties such as compressive strength, tensile strength, flexural strength, and elastic modulus at 7, 14, 28, and 90 days. The morphological investigations through SEM were performed for HPC with MK and compared with the control mix. It was observed that the inclusion of MK resulted in lower workability owing to its finer particle sizes. The optimized inclusion of 10% MK has shown improvement in the properties of HPC; however, increased curing enhanced the properties of HPC even at lower w/b ratios.

**Keywords:** High-performance concrete; w/b ratio; Metakaolin; Workability; Strength.

## 1. INTRODUCTION

High-performance concrete (HPC) is a concrete with a strength higher than 60 MPa with enhanced properties manufactured to achieve the strength and serviceability requirements. The serviceability requirements in control concrete (CC) are not better compared to HPC (Norhasri *et al.* 2016). The HPC exhibits amended properties compared to CC regarding high workability, pumpability, strength, higher early-age strength, and improved durability (Vejmelkova *et al.* 2010; Tafraoui *et al*. 2016). Such enhanced properties in HPC can be achieved by either SCM or chemical admixtures (Poon *et al.* 2006; Sankar and Ramadoss, 2023). The SCM reduces the production of Ca(OH)2 resulting in lower heat of hydration, higher early age strength, better durability, etc., whereas chemical admixtures improve the workability of concrete. The use of mineral admixtures in HPC has improved drastically with advancements in the construction industry, owing to the economy, sustainability, and energy savings. The excessive emission of $CO_2$ during cement production eventually supported the usage of mineral admixtures (Jagan and Neelakantan, 2021). Few mineral admixtures, such as metakaolin, and GGBS effectively enhance the concrete properties promoting excessive utilization of HPC in a real-time application (Swaminathen *et al.* 2021; Bahmani and Mostofinejad, 2022). Similar to mineral admixtures, chemical admixtures support the HPC without affecting its fresh-state properties. The decrease in the w/b ratio is the critical parameter to enhance the properties of HPC; however, such a reduced w/b ratio might reduce the mixing ability of HPC. The chemical admixture's relatively super plasticizers adequately improve the workability of HPC at lower w/b ratios, without compensating strength and serviceability requirements. Metakaolin (MK), is one such Supplementary cementitious material (SCM)/mineral admixture obtained through the calcination of kaolin clay. China has abundant kaolin clay, a mixture of 15% of China clay and 10% mica (Sposito, 2016). It is a highly reactive pozzolanic material produced similar to cement but at a temperature in the range of 600 to 900 °C. Like cement, a substantial percentage of CO2 will be released but less than cement. The predominant characteristic of MK is its pozzolanic activity, wherein the MK interacts with Ca(OH)2 to form C-S-H. Several research studies have been conducted with MK as SCM in HPC; HPC with 20, 40, and 60% of MK exhibit strengths of 98.5, 93.8, and 62.3% of CC at 28 days, but optimizing at 20%, increased the strength by 101, 102, and 104% of CC at 60, 90 and 180 days. The SiO2 and Al2O3 interact with cement products to form C-S-H which improves strength at later ages (He *et al.* 2023).

MK, fly ash, and natural pozzolan were used as SCMs and observed reduced workability with an increase in the SCM, as the surface area of SCM was higher. The concrete mix with MK and fly ash shows higher strength owing to the finer particle size that acts as a micro-filler

between cement particles and improves pozzolanic activity (Hakeem *et al.* 2022). The blended use of MK with waste glass in high-performance self-compacting concrete reduced the workability by 2 to 6% owing to the higher surface of MK and glossy surface of waste glass. The optimized use of 10% of MK with waste glass shows 16% strength enhancement compared to CC (Sobuz *et al.* 2023). The production of low-impact HPC with MK, ground granulated blast-furnace slag (GGBS), and fly ash (FA) with 15% constant silica fume show that the slump was lessened by 15% and strength was enhanced by 5% at 28 days and 3.7% at 90 days (Abdellatief *et al*. 2023). The researchers also used MK and MgO to investigate the flexural strength of HPC and observed 7.4% and 9.1% enhancement in strength with 5% of MK and 10% of MgO at 7 and 28 days. It was also inferred that the addition of MgO beyond 10% covers cement, inhibiting the hydration and thus resulting in strength reduction (Zhang *et al.* 2022). The review on the microstructure of SCM inferred that optimized (20%) use of MK shows supplementary C-S-H formation that densifies the concrete microstructure and improves the properties of HPC (Bahmani and Mostofinejad, 2022). The optimized use of metakaolin to 10% at 0.26 w/b ratio produces concrete with a higher compressive strength of 89 MPa. The blended use of 12.5% of RHA and 7.5% shows 26.75% more strength than CC owing to the high pozzolanic activity of RHA and MK and the micro-filling ability that lessens the pore volume (Swaminathen *et al*. 2021). The use of less reactive MK to produce HPC at various w/b ratios reveals that the strength of HPC lowers at higher w/b ratios, and the HPC mix with 10% of MK tends to perform better. The filling ability and pozzolanic activity of MK improve the strength of HPC (Salimi *et al.* 2020).

The excess production and use of cement results in the excess release of CO2 and the need for suitable new construction methodology for high-rise construction without comprising serviceability requirements promotes the research attribute towards the HPC. The research on the use of advanced materials will create a new archetype in the construction sector for its intended applications of HPC. Extensive research in terms of strength and durability has been conducted with MK as SCM, however, only minimal studies encompass the long-term effect of MK in improving the properties of HPC. This study investigates the influence of MK in enhancing the long-term mechanical properties of the HPC.

## 2. MATERIALS AND METHODS

### 2.1 Raw Materials

In this research, CM and SCM, fine aggregate, coarse aggregate, potable water, and superplasticizer (SP) were utilized to manufacture HPC. 53 grade OPC with a specific gravity of 3.15 g/cc and a specific surface area of 335 kg/m2 was used as a binder (IS 4031 – Part I). Metakaolin (MK), a pozzolanic material obtained from heating Kaolin, an industrial by-product of paper sludge waste was used as SCM in the study. Table 1 depicts the oxide composition and properties of OPC and MK used in the study. Fig. 1 depicts the micrographs of MK and OPC and Fig. 2 depicts the XRD pattern of MK and OPC. The XRD pattern of OPC illustrated the peaks of C3S about 2θ = 28.2°, 31.5°, and 46.4°, peaks of C2S about 2θ = 29.6°, 33.4°, and 49.7°, peaks of C3A about 2θ = 31.8°, 37.6°, and 44.1°, peaks of C4AF about 2θ = 24.5°, 31.0°, and 54.3° and peaks of gypsum about 2θ = 10.5°, 21.8°, and 28.3°. The presence of SiO2 and Al2O3 was evident in the XRD pattern of MK, supporting the development of additional C-S-H gel.

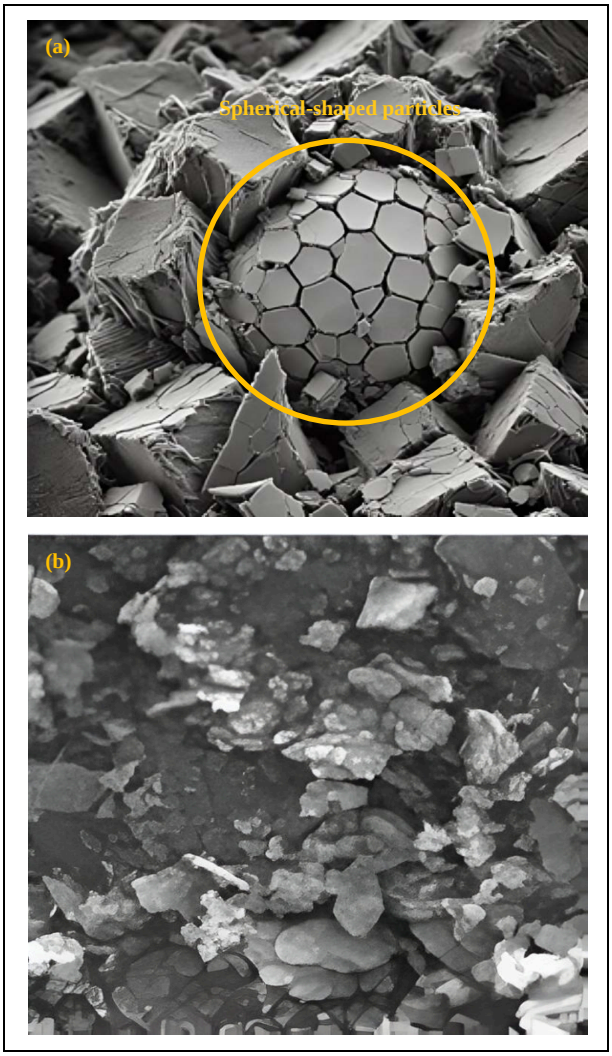



**Fig. 1: Microstructure of (a) OPC and (b) MK**

River sand with particle sizes relative to 2.36 mm ~ 4.75 mm having a specific gravity of 2.57, water absorption of 0.95%, and density of 1547 kg/m3 was utilized as fine aggregates, and river gravel with particle sizes relative to 10 mm ~ 20 mm having a specific gravity of 2.73, water absorption of 0.85% and density of 1709 kg/m3 was utilized as coarse aggregates (IS 2386 – Part

III). Conplast SP430 obtained from the local vendors having a specific gravity of 1.2 was used as SP and the potable water free from dust, grease, and impurities with basic pH was used in the research. Fig. 3 depicts the gradation curves of fine aggregate and coarse aggregate in the study.

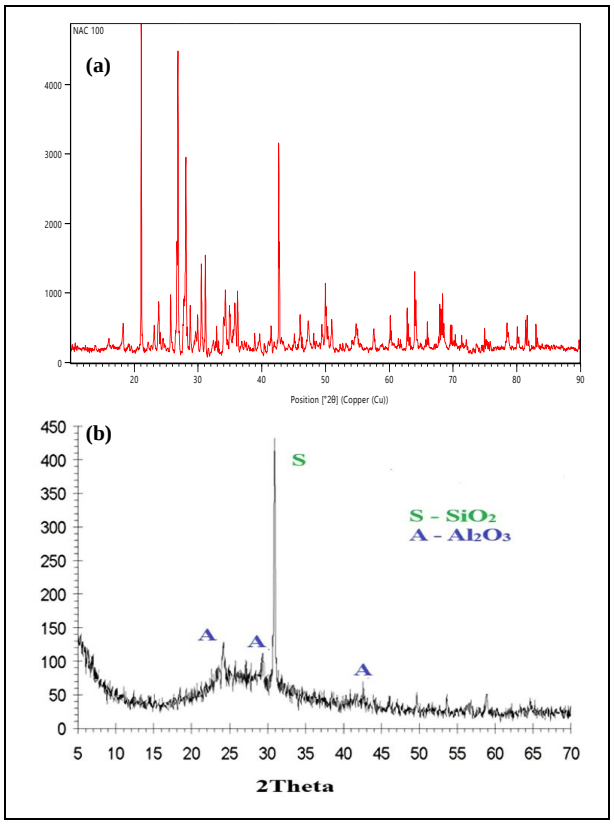



**Fig. 2: XRD pattern (a) OPC and (b) MK**

## 2.2 Concrete Mixtures

Four distinct samples were developed with two control mixes at both w/b ratios and two mixes with different proportions of MK at the same w/b ratios as per IS 10262 (2009). The HPC mixes were manufactured at two different w/b ratios to investigate their behavior at higher and lower w/b ratios. The first two control samples were prepared with OPC, fine aggregate, coarse aggregate, water, and SP at 0.3 and 0.45 w/b, while the third and fourth samples were prepared with OPC, fine aggregate, coarse aggregate, water, SP, and MK of different proportions (5, 10, 15, 20, 25, and 30%) as a substitute to cement at 0.3 and 0.45 w/b ratios. On a whole, 14 different concrete mixes were prepared for 4 distinct samples at 0.3 w/b and 0.45 w/b. The concrete mixtures are labeled as MxWBy, where 'Mx' represents the percentage of metakaolin, 'WB' represents the w/b ratio, and 'y' represents 0.3/0.45. The SP was dosed at 1% by weight of the binder for 0.3 w/b mixes. Table 1 shows the quantities of raw materials for the manufacture of HPC at both w/b ratios. The HPC mixes were prepared at 0.3 w/b and 0.45 w/b with 0 to 30% of MK at 5% intervals through the conventional mixing technique.

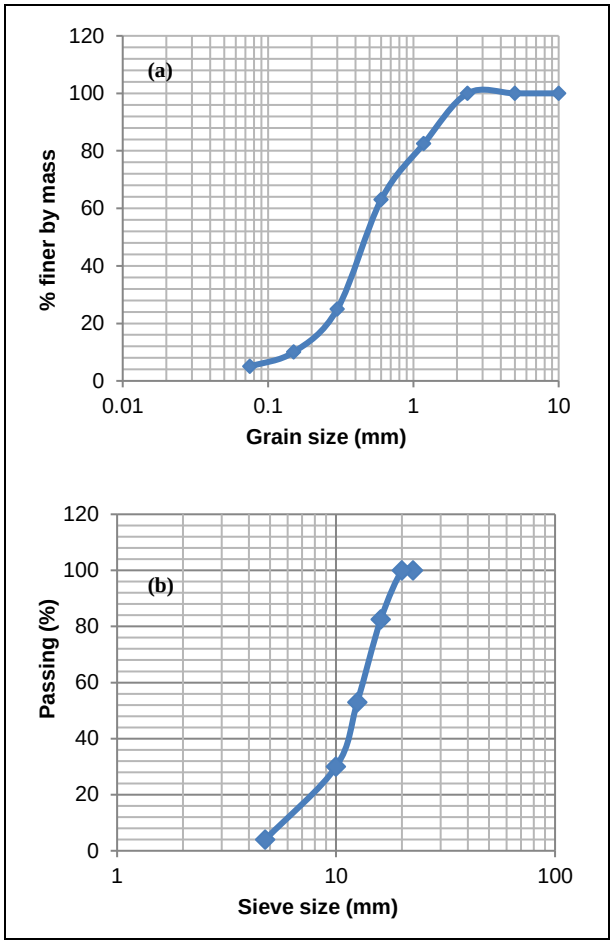



**Fig. 3: Gradation curves: (a) fine aggregate and (b) coarse aggregate**

**Table 1. Quantities of raw materials for manufacture of HPC**

| Mix No. | Mix ID | (kg/m$^3$) | | | | |
|---|---|---|---|---|---|---|
| | | Cement | MK | Fine Aggregate | Coarse Aggregate | Water |
| M1 | M0WB0.3 | 550 | 0 | 640 | 1075 | 165 |
| M2 | M0WB0.45 | 550 | 0 | 640 | 1075 | 247.5 |
| M3 | M5WB0.3 | 522.5 | 27.5 | 640 | 1075 | 165 |
| M4 | M10WB0.3 | 495 | 55 | 640 | 1075 | 165 |
| M5 | M15WB0.3 | 467.5 | 82.5 | 640 | 1075 | 165 |
| M6 | M20WB0.3 | 440 | 110 | 640 | 1075 | 165 |
| M7 | M25WB0.3 | 412.5 | 137.5 | 640 | 1075 | 165 |
| M8 | M30WB0.3 | 385 | 165 | 640 | 1075 | 165 |
| M9 | M5WB0.45 | 522.5 | 27.5 | 640 | 1075 | 247.5 |
| M10 | M10WB0.45 | 495 | 55 | 640 | 1075 | 247.5 |
| M11 | M15WB0.45 | 467.5 | 82.5 | 640 | 1075 | 247.5 |
| M12 | M20WB0.45 | 440 | 110 | 640 | 1075 | 247.5 |
| M13 | M25WB0.45 | 412.5 | 137.5 | 640 | 1075 | 247.5 |
| M14 | M30WB0.45 | 385 | 165 | 640 | 1075 | 247.5 |

### 2.3 Testing of Specimens

The manufactured HPC mixes were fabricated into cubes, cylinders, and prisms to evaluate the concrete properties. The HPC mixes were filled in three layers and vibrated to allow the concrete particles to settle without voids, and the top layer was smoothed using a trowel. The concrete mix was then allowed to be set for a day and cured under laboratory conditions to evaluate its properties. Fig. 4 depicts the experimental setup for the concrete testing. The HPC mixes at fresh state were tested for their workability using the compaction factor test as per IS 5515 (1983). The compressive strength (CS) of HPC mixes was evaluated with 150 mm cubes in accordance with IS 516 (1959). The tensile strength (TS) of HPC mixes was evaluated with 150 mm × 300 mm cylinders as per IS 5816 (1999). The flexural strength (FS) of HPC mixes was evaluated with 500 mm × 100 mm × 100 mm prisms as per IS 516 (1959). The elastic modulus (EM) of HPC mixes was evaluated with 150 mm × 300 mm cylinders as per IS 516 (1959).




**Fig. 4: Experimental setup: (a) CS (b) TS (c) FS and (d) EM**

## 3. RESULTS AND DISCUSSION

### 3.1 Workability

Fig. 5 depicts the workability of HPC mixes with different percentages of MK. It was observed that an increase in the MK decreases the workability of HPC. The workability of M3, M4, M5, M6, M7, and M8 was lowered by 1.17, 2.52, 5.88, 8.23, 9.41, and 11.76% compared to M1. The decrease in the workability is due to the increase in the fineness of MK. The finer particle size of MK increases the water demand, and thus decrease in the workability was observed with an increase in the MK (Khayat *et al.* 2019; Swaminathen *et al.* 2021). Moreover, a higher w/b ratio increases the workability of HPC mixes owing to the addition of higher water content. The workability of the HPC mix at 0.45 w/b ratio was 8% higher than the HPC mix at 0.3 w/b ratio. The workability of M9, M10, M11, M12, M13, and M14 was lowered by 1.09, 2.12, 5.21, 7.86, 8.91, and 10.94% compared to M2. The finer particle size of MK increases the water demand, and thus decrease in the workability was observed with an increase in MK (Amanjean *et al*. 2019).

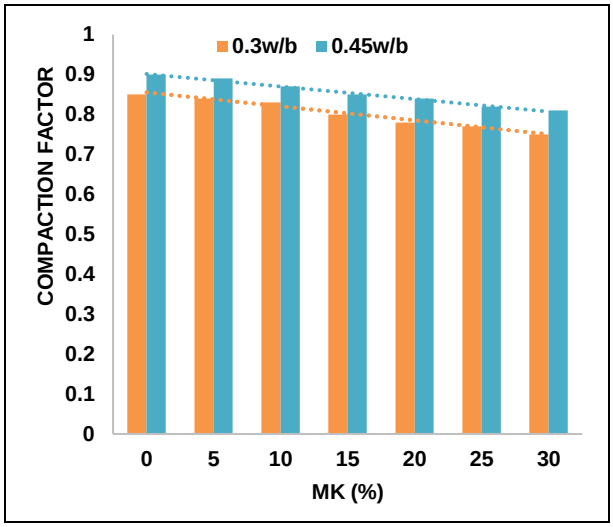



**Fig. 5: Workability of HPC**

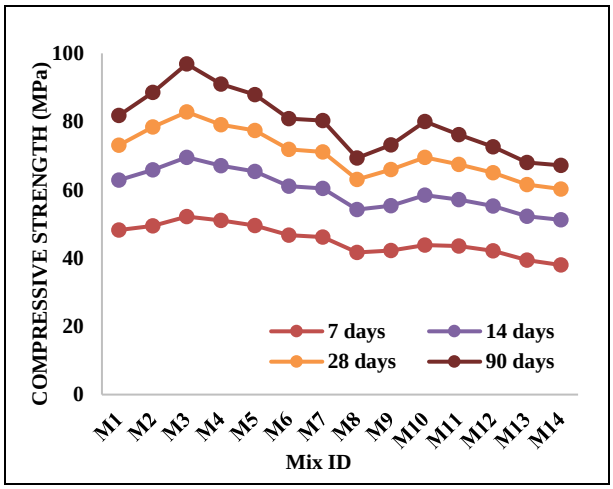



**Fig. 6: Compressive strength of HPC**

### 3.2 Compressive Strength

Fig. 6 depicts the CS of HPC mixes with different percentages of MK at 0.3 w/b. The CS of HPC increased with an increase in the MK up to 20%, but the increase was positive till 10%, thus optimizing the MK to 10%. Similarly, the CS of HPC with MK increases with increase in the curing ages. The CS of M3, M4, M5, and M6 were 2.36, 7.55, 5.50, and 2.59% higher than M1 at 7 days. At 14 days, the CS of M3, M4, M5, and M6 were 4.58, 9.65, 6.34, and 3.87% higher than M1, and at 28 days, the CS of M3, M4, M5, and M6 were 6.80,

11.75, 7.65, and 5.54% higher than M1. At 90 days, the CS of M3, M4, M5, and M6 were 7.62, 15.52, 10.05, and 6.88% higher than M1. The improvement in the strength of HPC mixes with MK can be attributed to the formation of additional C-S-H and C-A-S-H gel owing to the interaction between Al2O3 and SiO2 with Ca(OH)2, higher surface area of MK that quickens the hydration reaction and micro-filling ability of MK that reduces the pore volume and densifies the ITZ of the HPC (Poon *et al.* 2006; Abdellatief *et al*. 2023). However, the CS of M7 and M8 were lowered by 3.19 and 4.22% at 7 days, 2.84 and 3.88% at 14 days, 1.70 and 2.75% at 28 days, and 1.27 and 1.88% at 90 days. The reduction in the strength beyond optimal replacement of MK was the attribute of the clinker dilution effect. The dilution effect means the vice-versa of the synergic effect of SCM ensuing from the higher substitution of MK. The decrease in strength reduction at higher curing ages was due to the availability of suitable source of moisture for the hydration process. Such attribute strengthens the C-S-H and improves the CS of the HPC (Dushimimana *et al*. 2021).

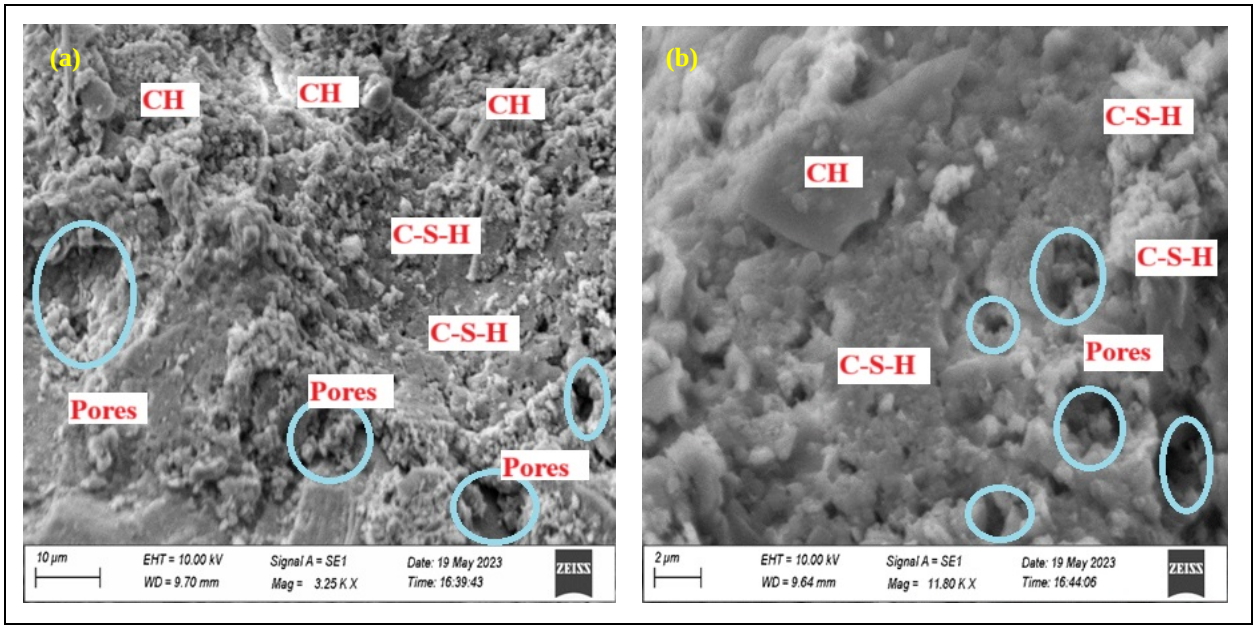



**Fig. 7: Microstructure of HPC with 0% MK (0.3 w/b) (a) 10 µm and (b) 2 µm**

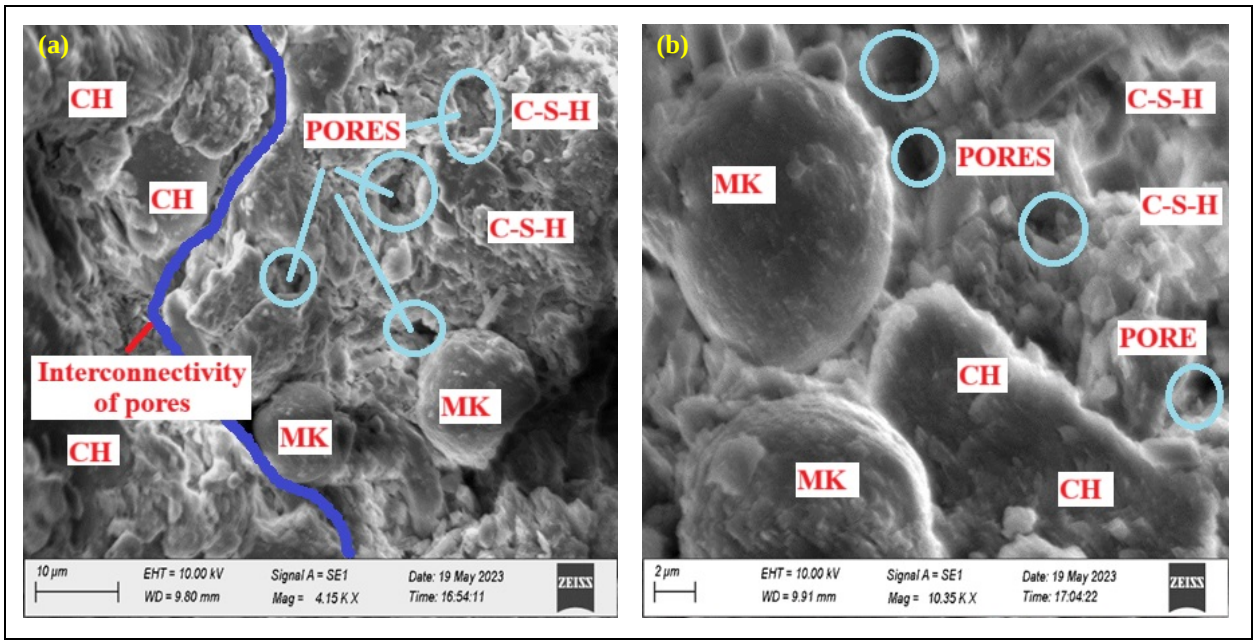



**Fig. 8: Microstructure of HPC with 10% MK (0.3 w/b) (a) 10 µm and (b) 2 µm**

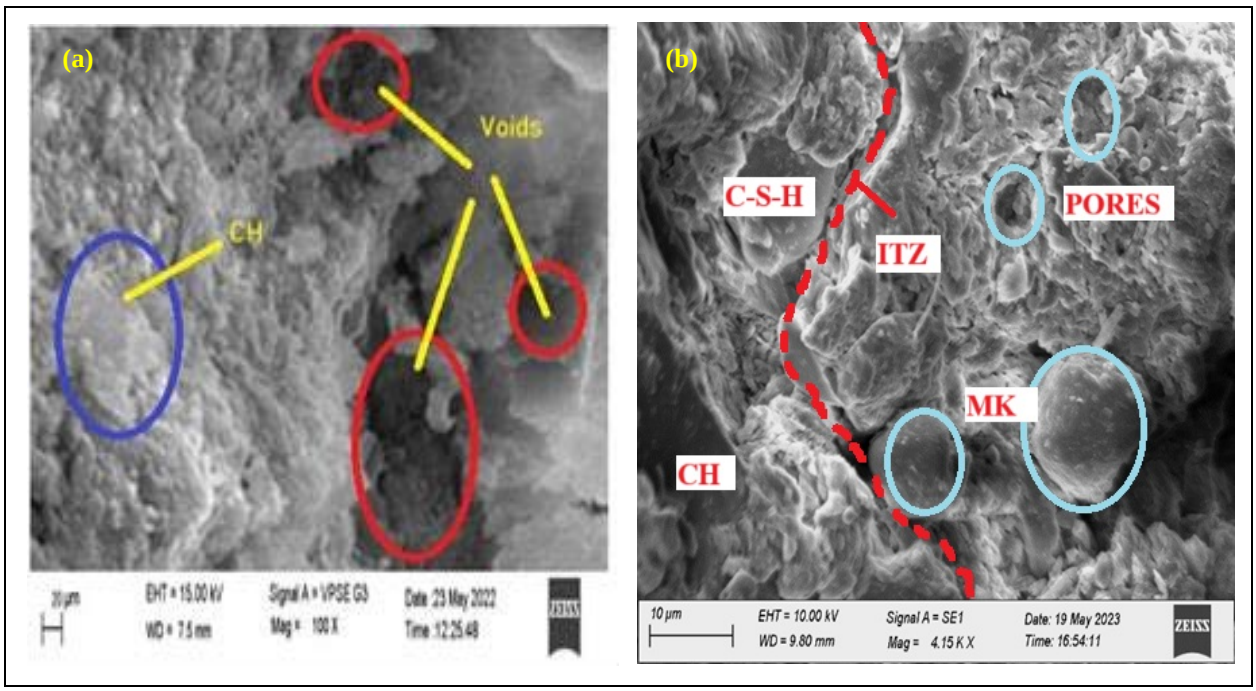



**Fig. 9: Microstructure of HPC with 0% MK (0.45 w/b) (a) 20 µm and (b) 10 µm**

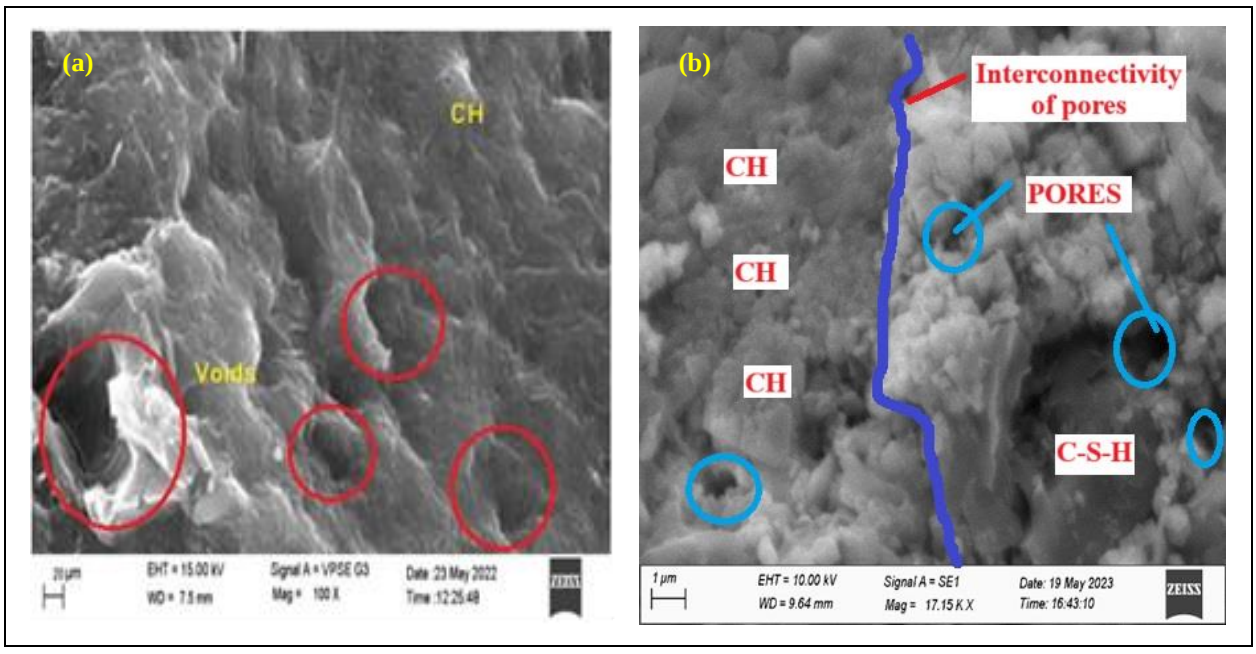



**Fig. 10: Microstructure of HPC with 10% MK (0.45w/b) (a) 20 µm and (b) 1 µm**

Similar to the 0.3 w/b ratio, the CS of HPC with MK was optimized at 10% for 0.45 w/b, and CS increases with an increase in the curing ages. At higher w/b ratios, the CS tends to reduce. The CS of M9, M10, M11, and M12 were 1.35, 5.03, 4.32, and 1.11% higher than M2 at 7 days. At 14 days, the CS of M9, M10, M11, and M12 were 2.06, 7.19, 5.17 and 1.86% higher than M2 and at 28 days, the CS of M9, M10, M11, and M12 were 4.34, 9.35, 6.50, and 3.06% higher than M2. At 90 days, the CS of M9, M10, M11, and M12 were 5.20, 12.29, 8.98, and 4.45% higher than M2. However, the CS of M13 and M14 tend to reduce, but the percentage decrease tends to reduce at higher curing ages. The CS of M13 and M14 were decreased by 5.38% and 8.78% at 7 days, 3.56% and 5.55% at 14 days, 2.43% and 4.44% at 28 days and 1.98% and 3.14% at 90 days. At a higher w/b ratio, the higher water content in the mix forms pore-connectivity, which on evaporation, forms void and thereby resulting in the reduced strength in the HPC (Amanjean *et al.* 2019).

Fig. 7 depicts the microstructure of HPC with 0% MK at 0.3 w/b. Fig. 8 depicts the microstructure of HPC with 10% MK at 0.3 w/b. Fig. 9 depicts the microstructure of HPC with 0% MK at 0.45 w/b. Fig. 10 depicts the microstructure of HPC with 10% MK at 0.45 w/b. It was observed that the formation of voids was more in 0.45 w/b mixes due to pore connectivity resulting from the addition of excess water. The addition of MK results in the formation of additional C-S-H gel and reduces the pore volume of HPC that could be visible in the microstructure. The microstructure of HPC shows evidence of Ca(OH)2, C-S-H, and unhydrated particles. At higher curing periods, the microstructure of HPC becomes densified owing to the formation of supplementary C-S-H ensuing from the pozzolanic reaction. The pozzolanic reactions densify the microstructure of HPC and condense the thickness of ITZ. The ITZ of the HPC with MK can be observed in Figures 7, 8, and 9. The compactness of ITZ with the addition of MK increases depicting the development of additional hydrated products. However, at a higher w/b ratio, the ITZ was observed with voids owing to the pore volume developed with excess addition of water. The addition of optimized MK in a 0.45 w/b ratio shows minimum voids in the ITZ with fewer cracks and additional hydrated products.

## 3.3 Tensile Strength

Fig. 11 depicts the TS of HPC mixes with different percentages of MK at 0.3 w/b. The TS of HPC increases with an increase in the MK up to 20%, but the increase was positive till 10%, thus optimizing the MK to 10%. Similarly, with an increase in the curing ages, the TS of HPC with MK increases eventually. The TS of M3, M4, M5, and M6 were 2.81%, 7.25, 5.16, and 2.92% higher than M1 at 7 days. At 14 days, the TS of M3, M4, M5, and M6 were 3.92, 8.31, 5.58, and 3.56% higher than M1, and at 28 days, the TS of M3, M4, M5, and M6 were 5.04, 9.38, 6.24, and 4.41% higher than M1. At 90 days, the TS of M3, M4, M5, and M6 were 5.46, 11.34, 7.47, and 5.01% higher than M1. The improvement in the TS of HPC with MK can be attributed to the formation of additional C-S-H and C-A-S-H gel, a higher surface area of MK which quickens the hydration reaction and micro-filling ability of MK which tends to reduce the pore volume and densifies the ITZ of the HPC (Borosnyoi, 2016). However, the TS of M7 and M8 was lowered by 3.25% and 3.77% at 7 days, 3.07% and 3.59% at 14 days, 2.50% and 3.03% at 28 days and 2.29% and 2.60% at 90 days. The reduction in the TS of MK beyond optimal replacement was the attribute of the clinker dilution effect. The dilution effect means the vice versa of the synergic effect of SCM ensuing from the higher replacement of MK. The decrease in the strength reduction upon prolonged curing was due to the suitable source of moisture available for the hydration process. Such attribute strengthens the C-S-H and improves the TS of HPC (Abdellatief *et al*. 2023; Sobuz *et al.* 2023).

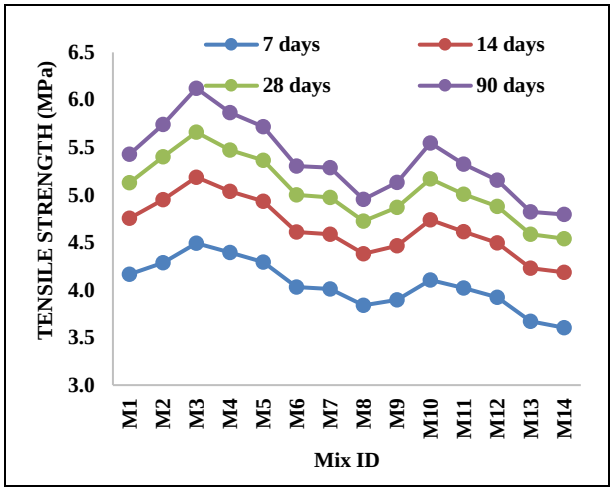



**Fig 11: Tensile strength of HPC mixes**

Similar to the 0.3 w/b, the TS of HPC with MK was optimized at 10% for 0.45 w/b ratio mixes, and TS increases with an increase in the curing ages. At higher w/b ratio, the TS tends to decrease. The TS of M9, M10, M11, and M12 were 1.50, 6.48, 4.59, and 2.20% higher than M2 at 7 days. At 14 days, the TS of M9, M10, M11, were M12 was 1.86, 7.55, 5.02, and 2.57% higher than M2 and at 28 days, the TS of M9, M10, M11, and M12 were 3.01, 8.63, 5.68, and 3.17% higher than M2. At 90 days, the TS of M9, M10, M11, and M12 were 3.45,10.64, 6.94, and 3.87% higher than M2. However, the TS of M13 and M14 tend to reduce, but the percentage decrease tends to reduce at higher curing ages. The TS of M13 and M14 was reduced by 4.36% and 6.10% at 7 days, 3.45% and 4.45% at 14 days, 2.88% and 3.89% at 28 days and 2.66% and 3.24% at 90 days. The reduction at higher w/b ratio was attributed to the pore volume ensuing from the connectivity of water molecules upon evaporation (Amanjean *et al*. 2019).

## 3.4 Flexural Strength

Fig. 11 depicts the FS of HPC mixes with different percentages of MK at 0.3 w/b. Similar to CS and TS, the FS of HPC increases with an increase in the MK up to 20%, but the increase was positive till 10%, thus optimizing the MK to 10%. Similarly, with the increase in the curing ages, the FS of HPC with MK increases eventually. The FS of M3, M4, M5, and M6 were 3.75, 19.87, 14.22, and 7.47% higher than M1 at 7 days. At 14 days, the FS of M3, M4, M5, and M6 were 4.85, 20.79, 17.05, and 15.48% higher than M1, and at 28 days, the FS of M3, M4, M5, and M6 were 5.97, 21.72, 17.63, and 16.22% higher than M1. At 90 days, the FS of M3, M4, M5, and M6 were 6.38, 23.41, 18.71, and 16.81% higher than M1. The justification for improvement in FS was similar to that of CS and TS. However, the FS of M7 and M8 was lowered by 8.17% and 8.66% at 7 days; 8.01%

and 8.50% at 14 days; 7.46% and 7.96% at 28 days, and 7.26% and 7.55% at 90 days The reduction in the FS of HPC beyond optimal replacement of MK was attributed to the clinker dilution effect. Also, the decrease in the FS reduction upon prolonged curing was due to the availability of ample moisture for the hydration process. Such attribute strengthens the C-S-H and improves the FS of HPC (Kaikea *et al.* 2014; Liu *et al*. 2022).

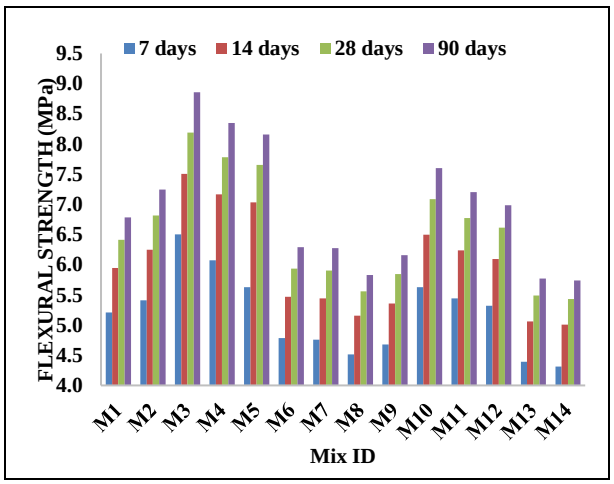



**Fig 12: Flexural strength of HPC mixes**

The FS of M9, M10, M11, and M12 were 3.44, 19.47, 17.00, and 15.11% higher than M2 at 7 days. At 14 days, the FS of M9, M10, M11, and M12 were 3.79, 20.66, 17.38, and 15.43% higher than M2 and at 28 days, the FS of M9, M10, M11, and M12 were 4.91, 21.59,17.95, and 15.95% higher than M2. At 90 days, the FS of M9, M10, M11, and M12 were 5.34, 23.31, 19.05, and 16.55% higher than M2. However, the FS of M13 and M14 tend to reduce, but the percentage decrease tends to reduce at higher curing ages. The FS of M13 and M14 was reduced by 2.73% and 4.49% at 7 days; 1.80% and 2.82% at 14 days; 1.22% and 2.25% at 28 days, and 1.01% and 1.58% at 90 days.

## 3.5 Elastic Modulus

Fig. 13 depicts the EM of HPC mixes with different percentages of MK at 0.3 w/b. The EM of M3, M4, M5, and M6 were 1.78, 6.48, 4.64, and 2.47% higher than M1 at 7 days. At 14 days, the EM of M3, M4, M5, and M6 were 2.53, 7.19, 4.92, and 2.90% higher than M1, and at 28 days, the EM of M3, M4, M5, and M6 were 3.30, 7.92, 5.36, and 3.47% higher than M1. At 90 days, the EM of M3, M4, M5, and M6 were 3.58, 9.25, 6.19, and 3.92% higher than M1. The justification for improvement in the EM directly depends on the improvement in the CS. The formation of additional C-S-H and strengthening of ITZ owing to the finer particle size of MK eventually improved the CS, and thus higher elastic modulus was observed. However, the EM of M7 and M8 was lowered by 2.32 and 2.67% at 7 days; 2.21 and 2.56% at 14 days; 1.82 and 2.18% at 28 days, and 1.68 and 1.89% at 90 days. The reduction in the EM of HPC beyond optimal replacement of MK can be attributed to the clinker dilution effect. Also, the attribute of a decrease in the EM reduction at higher curing ages was due to the ample moisture for the hydration process, thus strengthening the C-S-H (Tafraoui *et al*. 2016; Dushimimana *et al.* 2021).

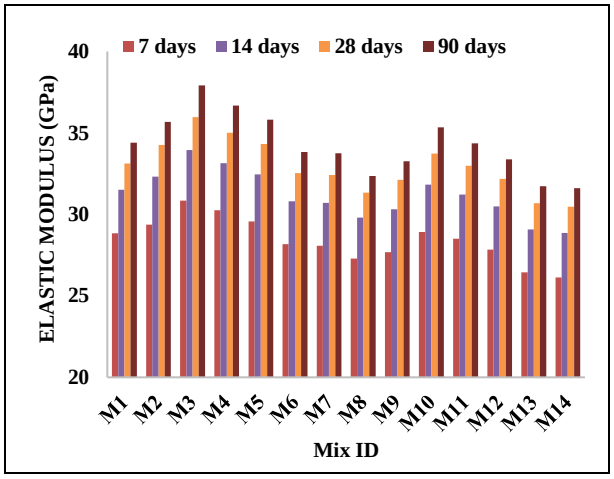



**Fig 13: Elastic modulus of HPC mixes**

The EM of M9, M10, M11, and M12 were 3.44, 19.47, 17.00, and 15.11% higher than M2 at 7 days. At 14 days, the EM of M9, M10, M11, and M12 were 3.79, 20.66, 17.38, and 15.43% higher than M2 and at 28 days, the EM of M9, M10, M11, and M12 were 4.91, 21.59, 17.95, and 15.95% higher than M2. At 90 days, the EM of M9, M10, M11, and M12 were 5.34, 23.31, 19.05, and 16.55% higher than M2. However, the EM of M13 and M14 tend to reduce, but the percentage decrease tends to reduce at higher curing ages. The EM of M13 and M14 were reduced by 2.73% and 4.49% at 7 days; 1.80% and 2.82% at 14 days; 1.22% and 2.25% at 28 days, and 1.01% and 1.58% at 90 days.

## 3.6 Regression Analysis

Fig. 14 depicts the correlation among various mechanical properties. Fig. 14 (a) depicts the correlation between CS and TS. It was found that a higher correlation was observed between CS and TS. The correlation equation between CS and TS at 0.3 w/b at 28 days was y = 0.059x+ 0.7902 with R2 = 0.9942. The correlation equation between CS and TS at 0.3 w/b at 90 days was y = 0.0505x + 1.2531 with R2 = 0.9917 and that at 0.45 w/b at 28 days was y = 0.068x + 0.4254 with R2 = 0.9890; at 0.45 w/b at 90 days it was y = 0.0585x + 0.8728 with R2 = 0.9929. Fig. 14 (b) depicts the correlation between CS and FS. It was found that a higher correlation was observed between CS and FS. The correlation equation between CS and FS at 0.3 w/b at 28 days was y = 0.1995x – 8.2572 with R2 = 0.8751 and that between CS and FS at 0.3 w/b at 90 days was y = 0.1562x – 4.8297 with R2 = 0.8677; at 0.45w/b at 28 days was y = 0.1887x – 6.0924 with R2 = 0.8095; at 0.45 w/b at 90

days was y = 0.1601x – 6.4713 with R2 = 0.8940. Fig. 14 (c) depicts the correlation between CS and EM. It was found that a higher correlation was observed between CS and EM. The correlation equation between CS and EM at 0.3 w/b at 28 days was y = 0.2969x + 11.667 with R2 = 0.9933 and that at 0.3 w/b at 90 days was y = 0.2504x + 13.712 with R2 = 0.9897; at 0.45 w/b at 28 days was y = 0.3585x + 8.7479 with R2 = 0.9866; at 0.45 w/b at 90 days was y = 0.3019x + 10.927 with R2 = 0.9825.

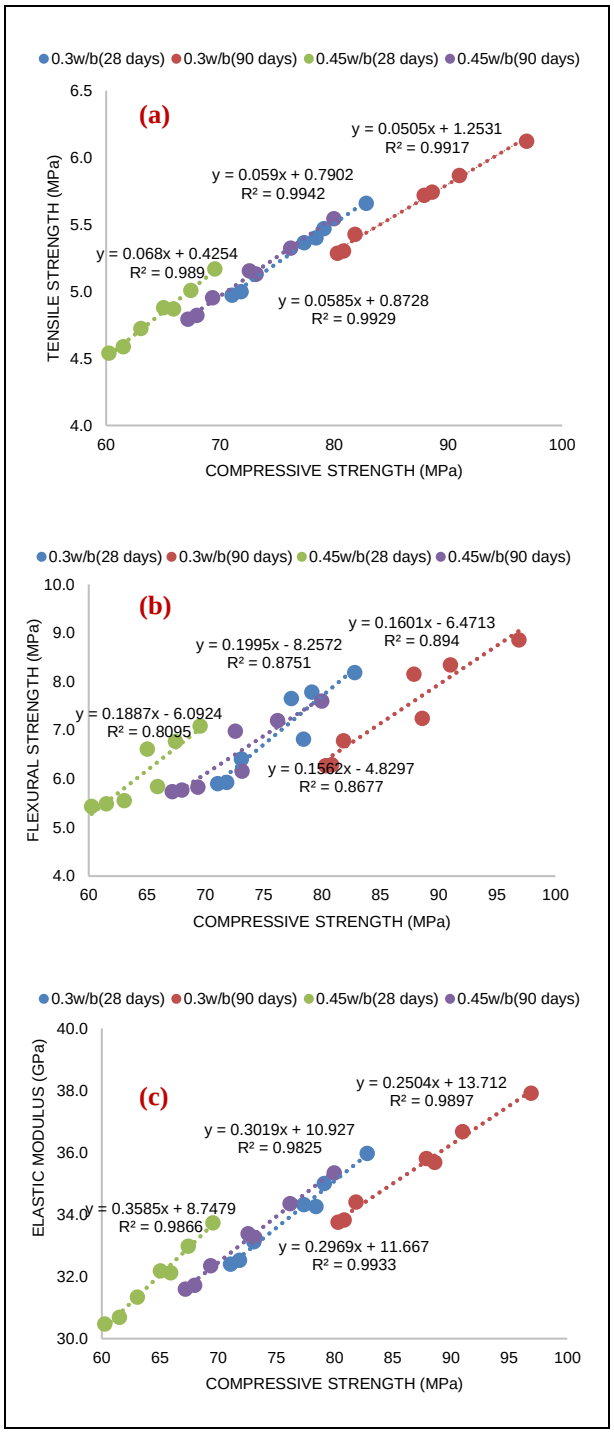



**Fig. 14: Correlation (a) CS vs. TS (b) CS vs. FS and (c) CS vs. EM**

## 4. CONCLUSION

This research encompasses the development of HPC with metakaolin at 0.3 and 0.45 w/b ratios. The OPC was substituted with MK up to 30% at intervals of 5%. The research discusses the influence of different proportions of MK on the long-term mechanical properties of HPC and the micro-structural investigations were also performed. The findings obtained through the research were provided as follows:

- The optimal replacement of MK was found to be 10%, beyond which it affects the properties of HPC. Also, an increase in the w/b ratio decreases the strength and elastic modulus of HPC.
- The HPC mixes exhibit better properties at a lower w/b ratio than at a higher w/b ratio. The higher w/b ratio mixes result in increased pore connectivity, which upon evaporation leaves voids resulting in the weaker matrix and thus inferior properties were observed.
- The workability of HPC lowers with higher proportions of MK and increases at higher w/b ratios; the workability of HPC lowers owing to the increase in the fineness of MK.
- The strength of HPC with 10% of MK at 0.3 w/b ratio was enhanced by 7.55, 9.62, 11.43, and 15.52% at 7, 14, 28, and 90 days; however, the strength of HPC with 10% MK at 0.45 w/b ratio was enhanced by 5.03, 7.19, 9.35, and 12.29% at 7, 14, 28, and 90 days. MK reacts with Ca(OH)2 to form additional C-S-H, and the micro-filling ability of MK densifies the micro-structure and improves the strength of HPC.
- Correlation analysis established among various mechanical properties at both w/b ratios shows a higher regression factor in the range of 0.9 to 1.0.
- The microstructure of HPC with MK at 0.3 w/b ratio shows densified C-S-H gel with reduced pore volume, while the microstructure of HPC with MK at 0.45 w/b ratio exhibit higher pore volume resulting from the connectivity of water molecules in the mixes.

## FUNDING

This research received no specific grant from any funding agency in the public, commercial, or not-for-profit sectors.

## CONFLICTS OF INTEREST

The authors declare that there is no conflict of interest.

## COPYRIGHT

This article is an open-access article distributed under the terms and conditions of the Creative Commons Attribution (CC BY) license (http://creativecommons.org/licenses/by/4.0/).

## REFERENCES

Abdellatief, M., Al-Tam, S. M., Elemam, W. E., Alanazi, H., Elgendy, G. M. and Tahwia, A. M., Development of ultra-high-performance concrete with low environmental impact integrated with metakaolin and industrial wastes, *Case Stud. Constr. Mater.,* 18, e01724(2023). https://doi.org/10.1016/j.cscm.2022.e01724

Amanjean, E. N., Mouret, M. and Vidal, T., Effect of design parameters on the properties of ultra-high-performance fibre-reinforced concrete in the fresh state, *Constr. Build. Mater.*, 224, 1007-1017(2019). https://doi.org/10.1016/j.conbuildmat.2019.07.284

Bahmani, H. and Mostofinejad, D., Microstructure of ultra-high-performance concrete (UHPC)–a review study, *J. Build. Eng.*, 50, 104118 (2022). https://doi.org/10.1016/j.jobe.2022.104118

Borosnyoi, A., Long-term durability performance and mechanical properties of high-performance concretes with combined use of supplementary cementing materials, *Constr. Build. Mater.,* 112, 307-324(2016). https://doi.org/10.1016/j.conbuildmat.2016.02.224

Dushimimana, A., Niyonsenga, A. A. and Nzamurambaho, F., A review on strength development of high-performance concrete, *Constr. Build. Mater.*, 307, 124865(2021). https://doi.org/10.1016/j.conbuildmat.2021.124865

Hakeem, I. Y., Althoey, F. and Hosen, A., Mechanical and durability performance of ultra-high-performance concrete incorporating SCMs, *Constr. Build. Mater.,* 359, 129430(2022). https://doi.org/10.1016/j.conbuildmat.2022.129430

He, Z. H., Wang, B., Shi, J.Y., Liu, D. E., Liu, J., Wang, D. D. and Hu, Y. J., Drying shrinkage and microstructural evolution of concrete with high-volume and low-grade metakaolin, *J. Build. Eng*., 76, 107206(2023). https://doi.org/10.1016/j.jobe.2023.107206

IS 10262: Guidelines for Concrete Mix Design Proportioning, Bureau of Indian Standards, New Delhi, India, (2009).

IS 2386 (Part III): Methods of test for aggregates for concrete, Bureau of Indian Standards, New Delhi, India, (1963).

IS 4031 (Part I): Methods of Physical tests for Hydraulic Cement, Bureau of Indian Standards, New Delhi, India, (1996).

IS 516: Methods of test for strength of the concrete, Bureau of Indian Standards, New Delhi, India, (1959).

IS 5515: Specification for compaction factor apparatus, Bureau of Indian Standards, New Delhi, India, (1983).

IS 5816: Methods of test for split tensile strength of the concrete, Bureau of Indian Standards, New Delhi, India, (1999).

Jagan, S. and Neelakantan, T. R., Effect of silica fumes on mechanical and durability properties of concrete, *Int. Review Appl. Sci. Eng*., 12, 44-49(2021). https://doi.org/10.1556/1848.2020.00129

Kaikea, A., Achoura, D., Duplan, F. and Rizzuti, L., Effect of mineral admixtures and steel fiber volume contents on the behavior of high-performance fiber reinforced concrete, *Mater. Design*, 63, 493-499(2014). https://doi.org/10.1016/j.matdes.2014.06.066

Khayat, K. H., Meng, W., Vallurupalli, K. and Teng, L., Rheological properties of ultra-high-performance concrete—An overview, *Cem. Concr. Res.,* 124, 105828(2019). https://doi.org/10.1016/j.cemconres.2019.105828

Liu, H., Elchalakani, M., Yehia, S., Sadakkathulla, M. A., Xie, T. and Yang, B., The influences of metakaolin, w/b ratio and fibers on the properties of green-HFLWC, *Constr. Build. Mater.,* 361, 129664(2022). https://doi.org/10.1016/j.conbuildmat.2022.129664

Norhasri, M. M. S., Hamidah, M. S., Fadzil, A. M. and Megawati, O., Inclusion of nano metakaolin as additive in ultrahigh-performance concrete (UHPC), *Constr. Build. Mater*., 127, 167-175(2016). https://doi.org/10.1016/j.conbuildmat.2016.09.127

Poon, C. S., Kou, S. C. and Lam, L., Compressive strength, chloride diffusivity and pore structure of high-performance metakaolin and silica fume concrete, *Constr. build. mater.,* 20(10), 858-865(2006). https://doi.org/10.1016/j.conbuildmat.2005.07.001

Salimi, J., Ramezanianpour, A. M. and Moradi, M. J., Studying the effect of low reactivity metakaolin on free and restrained shrinkage of high-performance concrete, *J. Build. Eng.,* 28, 101053(2020). https://doi.org/10.1016/j.jobe.2019.101053

Sankar, B. and Ramadoss, P., Modelling the compressive strength of high-performance concrete containing metakaolin using distinctive statistical techniques, *Results Control Optim.*, 12, 100241(2023). https://doi.org/10.1016/j.rico.2023.100241

Sobuz, M. H. R., Meraz, M. M., Safayet, M. A., Mim, N. J., Mehedi, M. T., Farsangi, E. N., Shrestha, R. K., Arafin, S. A. K., Bibi, T., Hussain, M. S., Aftab, M. R., Sujon, K. P., Prince, P., Meraz, M. M. and Bhattacharya, B., Performance evaluation of high-performance self-compacting concrete with waste glass aggregate and metakaolin, *J. Build. Eng.*, 67, 105976(2023). https://doi.org/10.1016/j.jobe.2023.105976

Sposito, G., The Chemistry of Soil. 3rd Ed, Oxford University Press, New York, (2016).

Swaminathen, A. N., Kumar, C. V., Ravi, S. R. and Debnath, S., Evaluation of strength and durability assessment for the impact of Rice Husk ash and Metakaolin at High-Performance Concrete mixes, *Mater. Today: Proc.*, 47, 4584-4591 (2021). https://doi.org/10.1016/j.matpr.2021.05.449

Tafraoui, A., Escadeillas, G. and Vidal, T., Durability of the ultra-high performances concrete containing metakaolin, *Constr. Build. Mater.,* 112, 980-987(2016). https://doi.org/10.1016/j.conbuildmat.2016.02.169

Vejmelkova, E., Pavlikova, M., Keppert, M., Keršner, Z., Rovnaníková, P., Ondráček, M., Sedlmajer, M. and Černý, R., High-performance concrete with Czech metakaolin: Experimental analysis of strength, toughness and durability characteristics, *Constr. Build. Mater.*, 24(8), 1404-1411(2010). https://doi.org/10.1016/j.conbuildmat.2010.01.017

Zhang, B., Ji, T., Ma, Y. and Zhang, Q., Effect of metakaolin and magnesium oxide on flexural strength of ultra-high-performance concrete, *Cem. Concr. Compos*., 131, 104582(2022). https://doi.org/10.1016/j.cemconcomp.2022.104582